Timur M. Gamilov, Philippe Yu. Kopylov, Roman A. Pryamonosov, and Sergey S. Simakov*

# Virtual fractional flow reserve assessment in patient-specific coronary networks by 1D hemodynamic model

**Abstract:** Atherosclerotic diseases of coronary vessels are the main reasons of myocardial ischemia. The value of the fractional flow reserve (FFR) factor is the golden standard for making decision on coronary network surgical treatment. The FFR measurements require expensive endovascular diagnostics. We propose a non-invasive method of the virtual FFR assessment in patient-specific coronary network based on angiography and computer tomography data. Also we analyze sensitivity of the model to the heart stroke volume.

**Keywords:** Fractional flow reserve, coronary circulation, computational hemodynamics.

**MSC 2010:** 76Z05, 92C35, 92C50

DOI: 10.1515/rnam-2015-0024
Received July 30, 2015; accepted August 25, 2015

Atherosclerotic diseases of coronary vessels are the main reasons of myocardial ischemia frequently resulting in disability or death. The basic methods of medical treatment assume invasive endovascular intervention, i.e. bypassing or balloon angioplasty with stenting. The use of these methods is limited in some cases due to personal counterindications or low effectiveness. Decision on type of treatment is based on the estimate of stenosis of the diseased vessels and its impact on myocardial perfusion.

The vascular occlusion factor (VOF) defined as the relative lesion cross-sectional area decrease based on angiography analysis has been used recently as a measure of hemodynamic significance of the stenosis. The VOF values over 70% was generally recommended as a threshold for a surgical intervention. The VOF values below 50% was considered as not significant for hemodynamics. Nevertheless, in some cases severe occlusions have no hemodynamic impact whereas relatively small occlusions cause acute myocardial infarction. The key factors for hemodynamic significance of the stenosis may include collateral network development, hemostasis, vascular autoregulation. The modern criterion of the endovascular surgical treatment efficiency is fractional flow reserve (FFR) [1, 9]. FFR is calculated as the ratio of mean pressure distal a stenosis to mean aortic pressure under conditions of vasodilator administration [8, 20]. The value of FFR below 80% is generally recommended as a threshold for a surgical intervention. In such approach one estimates both anatomical and physiological significance of the stenosis. The FFR based assessment has reduced significantly the number of costly operations with high risks. Also, the number of incidences caused disability or death has decreased [20].

The invasive measurements of FFR are regularly performed by endovascular ultrasound catheter [1]. It requires expensive and invasive endovascular intervention. Contemporary non-invasive methods of FFR estimate are based on modelling 3D blood flow in the local region of the studied vessel [3, 14, 21]. This estimate is also referred to as virtual FFR. The method was subjected to criticism [10, 19] due to bad posedness of upstream and downstream boundary conditions, rigid wall approximation for the vessel's tissue, large computational cost, local region for computational domain, general difficulties in parameters fitting. One-

**Timur M. Gamilov, Philippe Yu. Kopylov, Roman A. Pryamonosov:** Institute of Numerical Mathematics of the RAS, Moscow 119333, Russia
**Timur M. Gamilov, Roman A. Pryamonosov:** Moscow Institute of Physics and Technology, Dolgoprudny 141700, Russia
**Philippe Yu. Kopylov:** I. M. Sechenov First Moscow State Medical University, Moscow 119991, Russia
***Corresponding Author: Sergey S. Simakov:** Institute of Numerical Mathematics RAS, Moscow 119333, Russia. Moscow Institute of Physics and Technology, Dolgoprudny 141700, Russia. E-mail: simakov.ss@mipt.ru

dimensional (1D) hemodynamics has been rarely used for the virtual FFR assessment. In [4] excellent fitting between measured and computed FFR was achieved using 1D physiologically correct coronary network domain. The 1D approach was also applied in [15] to study FFR sensitivity to the heart ejection variability (peak ejection and heart rate) using individual 1D coronary network domain.

Using our experience of hemodynamics modelling in patient-specific vascular networks [6, 15], we propose an improved technique for personalized non-invasive virtual FFR assessment on the basis of 1D hemodynamics. The input data includes angiography expert analysis and CT-scans. The other parameters were set according to well-known physiologically correct ranges. We consider two patient-specific cases with multiple coronary stenosis. The 1D network is constructed on the basis of individual CT-scans and personalised virtual FFR is computed. We demonstrate that our approach is capable to predict FFR with acceptable accuracy. Thus this technique is suitable for the bedside applications. We also study the virtual FFR sensitivity to the stroke volume variability that corresponds to the physical stress test. We observe substantial decrease of the FFR value during increased heart ejection. This phenomenon should be taken into account in endovascular treatment planning.

# 1 Materials and methods

## 1.1 Mathematical model of coronary circulation

The model of blood flow in coronary vascular network considers unsteady viscous incompressible fluid flow through the 1D network of elastic tubes [13]. It takes into account systemic arteries and veins with emphasis on patient-specific coronary circulation. The model is modified by active vessel wall response (autoregulation) function according to [12]. In this section we just present essential outlines of the model, for details we refer to [12, 13, 16]. The flow in every vessel is described by mass and momentum balances

$$\frac{\partial S_k}{\partial t} + \frac{\partial (S_k u_k)}{\partial x} = 0 \tag{1.1}$$

$$\frac{\partial u_k}{\partial t} + \frac{\partial (u_k^2/2 + p_k/\rho)}{\partial x} = f_{\text{fr}}(S_k, u_k) \tag{1.2}$$

where $k$ is the index of the vessel, $t$ is the time, $x$ is the distance along the vessel counted from the vessel junction point, $\rho$ is the blood density (constant), $S_k(t, x)$ is the vessel cross-section area, $p_k$ is the blood pressure, $u_k(t, x)$ is the linear velocity averaged over the cross-section, $f_{\text{fr}}$ is the friction force. The elastic properties of the vessel wall material are presented as $p_k(S_k)$ relationship

$$p_k(S_k) - p_{\star k} = \rho c_k^2 f(S_k) \tag{1.3}$$

where $f(S)$ is the monotone S-like function

$$f(S_k) = \begin{cases} \exp(\eta_k - 1) - 1, & \eta_k > 1 \\ \ln \eta_k, & \eta_k \leqslant 1 \end{cases} \tag{1.4}$$

while $p_{\star k}$ is the pressure in the tissues surrounding the vessel, $c_k$ is the velocity of small disturbances propagation in the wall, $\eta_k = S_k/S_{0k}$, $S_{0k}$ is the unstressed cross-sectional area.

At the vessels junctions the Poiseuille's pressure drop condition and the mass conservation condition are applied

$$p_k\left(S_k\left(t, \tilde{x}_k\right)\right) - p_{\text{node}}^l(t) = \varepsilon_k R_k^l S_k\left(t, \tilde{x}_k\right) u_k\left(t, \tilde{x}_k\right), \quad k = k_1, k_2, \ldots, k_M \tag{1.5}$$

$$\sum_{k=k_1,k_2,\ldots,k_M} \varepsilon_k S_k\left(t, \tilde{x}_k\right) u_k\left(t, \tilde{x}_k\right) = 0 \tag{1.6}$$

where $M$ is the number of the connected vessels, $\{k_1, \ldots, k_M\}$ is the range of the indices of the connected vessels, $R_k$ is the hydraulic resistance of the vessel, $p_{\text{node}}(t)$ is the pressure at the junction point, $\varepsilon = 1$, $\tilde{x}_k = L_k$ for incoming vessels, $\varepsilon = -1$, $\tilde{x}_k = 0$ for outgoing vessels.

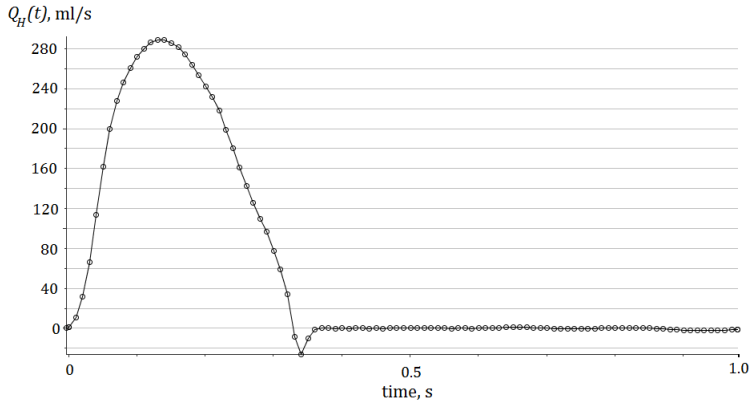


**Figure 1.** Aortic blood flow time profile.

At the terminal point of the venous system ($x = x_H$) the pressure $p_H = 8$ mmHg is set as the boundary condition

$$p_H(t, x_H) = p_H. \tag{1.7}$$

At the entry point of the aorta the blood flow is assigned as the boundary condition

$$u(t, 0)\, S(t, 0) = Q_H(t)\,. \tag{1.8}$$

Here function $Q_H(t)$ for normal conditions corresponds to heart rate 1 Hz and stroke volume 65 ml [7] (see Fig. 1).

Autoregulation impact is essential for the arterial part. We include it in the model as dependence of $c_k$ in (1.3) on time-averaged pressure $\overline{p}_k$ [12]. The value $c_k$ is updated every heart cycle according to the following algorithm

$$\frac{c_{k,\text{new}}}{c_{k,\text{old}}} = \sqrt{\frac{\overline{p}_{k,\text{new}}}{\overline{p}_{k,\text{old}}}} \tag{1.9}$$

where

$$\overline{p}_{k,\text{new}} = \frac{1}{(T_3 - T_2)l_k} \int_{T_2}^{T_3} \int_0^{l_k} p(x, t)\, \mathrm{d}x\, \mathrm{d}t, \qquad \overline{p}_{k,\text{old}} = \frac{1}{(T_2 - T_1)l_k} \int_{T_1}^{T_2} \int_0^{l_k} p(x, t)\, \mathrm{d}x\, \mathrm{d}t$$

while $l_k$ is the length of the $k$-th vessel; $T_1$, $T_2$, $T_3$, $T_4$ are the initial moments of the successive cardiac cycles. Actual value of $c_k$ is calculated as

$$c_k = c_{k,\text{old}} + y \frac{t - T_3}{T_4 - T_3}(c_{k,\text{new}} - c_{k,\text{old}}) \tag{1.10}$$

where $0 \leqslant y \leqslant 1$ is the parameter reflecting the autoregulation response rate. We associate $y = 1$ with the normal case and $y = 0.1$ with impact of vasodilator administration.

Another important feature of coronary hemodynamics is compression of a part of coronary arteries during systole by myocard. Thus the main myocardial perfusion occurs during heart diastole [11]. According to this feature we modify (1.3) by setting $p_\star = P_{\text{ext}}^{\text{cor}}(t)$. The shape of the function $P_{\text{ext}}^{\text{cor}}(t)$ is similar to the heart outflow time profile presented in Fig. 1. Maximum value is normalised by the ventricular pressure. It is set to 120 mm Hg and 30 mm Hg for terminal vessels of left and right coronary artery, respectively. To simulate increased resistance we increase $R_k$ in (1.5) for all coronary vessels during systole. The values of $R_k$ during systole are taken 3 times higher than the values during diastole according to [17].

## 1.2 Patient-specific 1D vascular domain identification

In general, the vascular network is a 3D tubular network represented as a set of patient-specific CT scans. 1D hemodynamic models operate with a 3D graph layout with straight edges. This graph should have the

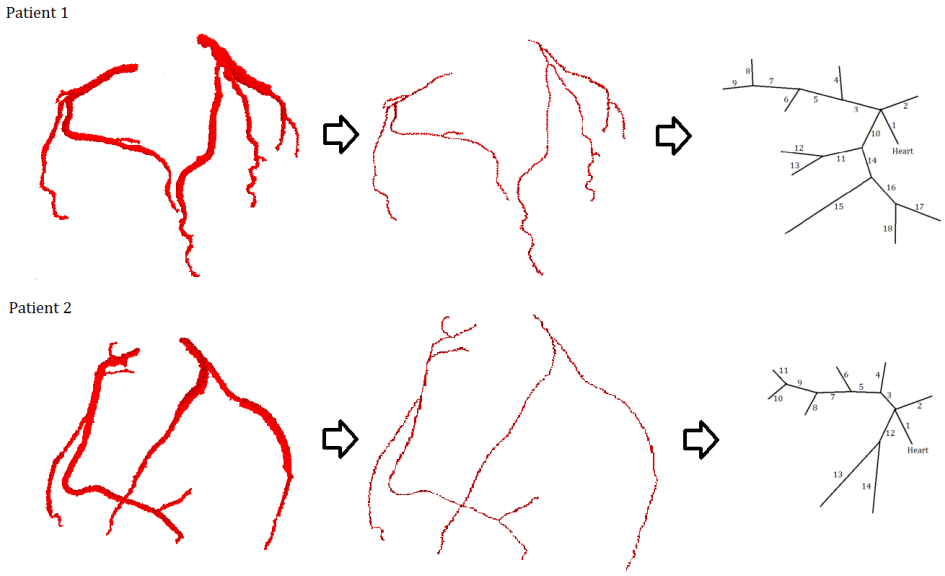


**Figure 2.** Reconstruction of patient-specific coronary networks. Left: 3D-structure obtained from CT scans; middle: centerlines; right: 1D network.

same topology as the original vascular network. Functional properties (elasticity, resistance, length, average diameter) should be attributed to edges and nodes of this structure.

The automatic method of CT scans processing [15] consists of four stages: aorta segmentation, computation of Frangi vesselness [5], ostia points detection and coronary vessel segmentation, skeletonization of segmented vessels and graph construction. Frangi vesselness filter is applicable even for discontinuous and moving structures which is especially important for coronary vessels segmentation. More details on implementation of these methods are given in [15].

Two anonymized patient cases with multiple stenosis of coronary arteries were studied in this work. Medical expert decision on the basis of CT and angiography data was used. Patient 1 was diagnosed with stenosis in three vessels: the proximal part (one third) of the left main coronary artery (LCA-1) with stenosis 55%, the middle one third of the left circumflex artery (LCX-1) with stenosis 80%, the middle one third of the left anterior descending artery (LAD-1) with stenosis 50%. Patient 2 was diagnosed with stenosis in two vessels: the proximal part (2 mm length) of the right main coronary artery (RCA-2) with stenosis 55%, the middle one third (2 cm length) of the left circumflex artery (LAD-2) with stenosis 80%. The value of FFR was measured in every case for every stenosis.

CT scan sets were used to construct the 1D network of coronary vessels for every patient according to the algorithm mentioned in the beginning of this section (see Fig. 2). Reduced anatomical attributes and functional parameters are summarized in Table 1. Functional parameters (stiffness and resistance) were assigned to the network with the help of pulse wave velocity studies [2] and other well-known medical and physiological literature [7, 11, 17].

The 1D structure of the arterial and venous coronary networks are considered to be the same. The parameters of the veins were adjusted to increase their blood capacity (see comments to Table 1). Each terminal artery is connected to a corresponding vein through a virtual terminal vessel with the following parameters: $l_k = 20$ cm, $d_k = 3$ cm, $c_k = 300\,\mathrm{cm\,s^{-1}}$, $R_k = 6000\,\mathrm{ba\,s\,cm^{-3}}$. Such vessels provide the realistic pressure drop between arteries and veins and simulates hydraulic resistance of microcirculation area.

Stenosis was modelled by separating diseased vessel into three parts: stenosed part, proximal part and distal part (see Fig. 4). The parameters of proximal and distal parts correspond to the parameters of the initial non-stenosed vessel. The parameters of stenosed part were modified as $S_{0,\mathrm{stenosed}} = (1-\alpha)S_0$, $R_{\mathrm{stenosed}} = R/(1-\alpha)^2$, where $\alpha$ is the stenosis fraction, $S_0$ is the cross-section of the initial vessel in the unstressed state, $R$

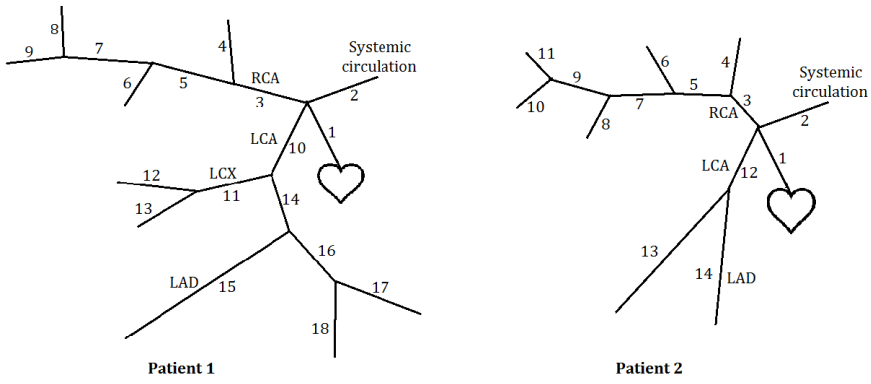


**Figure 3.** The structure of reconstructed arterial part based on two anonymous patient-specific data sets.

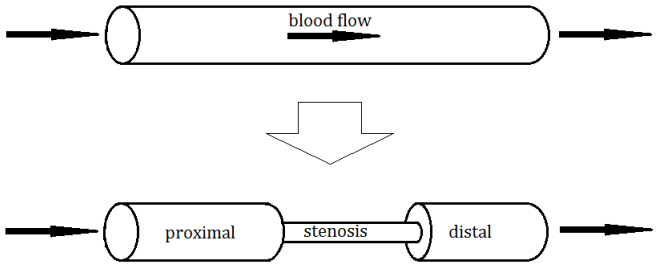


**Figure 4.** Model of stenosis in a 1D-vessel.

**Table 1.** The parameters of the arterial trees for patient 1 and patient 2: $k$ is the index of the vessel according to Fig. 3, $l_k$ is the length, $d_k$ is the diameter, $c_k$ is the stiffness (1.3), $R_k$ is the resistance (1.5). The veins are considered to have the same structure with $c_k$ lowered by 20%, $d_k$ doubled.

| $k$ | $l_k$, cm | $d_k$, mm | $c_k$, cm s$^{-1}$ | $R_k$, ba s cm$^{-3}$ | $k$ | $l_k$, cm | $d_k$, mm | $c_k$, cm s$^{-1}$ | $R_k$, ba s cm$^{-3}$ |
|---|---|---|---|---|---|---|---|---|---|
| Patient 1, arterial vessels | | | | | | | | | |
| 1 | 5.28 | 21.7 | 1050 | 20 | 10 | 0.59 | 3.6 | 950 | 720 |
| 2 | 60.0 | 25.1 | 840 | 20 | 11 | 6.1 | 3.0 | 950 | 720 |
| 3 | 2.72 | 3.1 | 1200 | 7200 | 12 | 2.05 | 1.17 | 950 | 720 |
| 4 | 1.44 | 1.31 | 1200 | 7200 | 13 | 1.75 | 1.21 | 950 | 720 |
| 5 | 1.40 | 2.73 | 1200 | 7200 | 14 | 1.39 | 3.8 | 950 | 720 |
| 6 | 6.75 | 1.52 | 1200 | 7200 | 15 | 12.1 | 2.05 | 950 | 720 |
| 7 | 5.01 | 2.50 | 1200 | 7200 | 16 | 5.4 | 1.91 | 950 | 720 |
| 8 | 1.27 | 1.19 | 1200 | 7200 | 17 | 0.38 | 1.01 | 950 | 720 |
| 9 | 5.65 | 0.157 | 1200 | 7200 | 18 | 2.62 | 1.19 | 950 | 720 |
| Patient 2, arterial vessels | | | | | | | | | |
| 1 | 5.28 | 21.7 | 1050 | 20 | 8 | 7.34 | 1.64 | 1200 | 7200 |
| 2 | 60.0 | 25.1 | 840 | 20 | 9 | 9.9 | 2.92 | 1200 | 7200 |
| 3 | 1.22 | 2.5 | 1200 | 7200 | 10 | 2.36 | 1.66 | 1200 | 7200 |
| 4 | 1.28 | 1.55 | 1200 | 7200 | 11 | 2.67 | 2.14 | 1200 | 7200 |
| 5 | 2.22 | 3.57 | 1200 | 7200 | 12 | 1.35 | 3.6 | 950 | 720 |
| 6 | 2.11 | 1.01 | 1200 | 7200 | 13 | 11.5 | 2.37 | 950 | 720 |
| 7 | 2.26 | 3.28 | 1200 | 7200 | 14 | 11.6 | 2.74 | 950 | 720 |

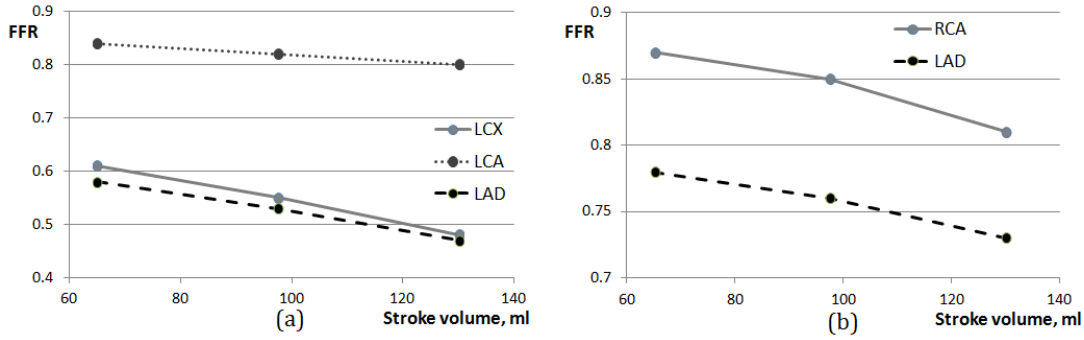


**Figure 5.** Virtual FFR calculated for three stroke volumes. (a) patient 1; (b) patient 2.

**Table 2.** Measured FFR and virtual FFR in different vessels: left anterior descending artery of patient 1 (LAD-1), left main coronary artery of patient 1 (LCA-1), left circumflex artery of patient 1 (LCX-1), left anterior descending artery of patient 2 (LAD-2), right main coronary artery of patient 2 (RCA-2).

| Vessel | Measured FFR | Virtual FFR | Difference |
|---|---|---|---|
| LAD-1 | 0.51 | 0.58 | +14% |
| LCA-1 | 0.72 | 0.84 | +17% |
| LCX-1 | 0.59 | 0.61 | +3% |
| LAD-2 | 0.74 | 0.78 | +5% |
| RCA-2 | 0.93 | 0.87 | −5% |

is the resistance of the initial vessel. The stenosed and non-stenosed cases were applied to vessels LAD-1, LCA-1, LCX-1, LAD-2, RCA-2 shown in Fig. 3. Parameter $\alpha$ was set in each case according to the above description.

## 2 Results

The virtual FFR is calculated as the ratio of average pressure in coronary artery distal to stenosis ($\overline{P}_{\text{dist}}$) to average aortic pressure ($\overline{P}_{\text{aortic}}$) during vasodilator administration

$$FFR = \frac{\overline{P}_{\text{dist}}}{\overline{P}_{\text{aortic}}}. \tag{2.1}$$

Vasodilator administration is simulated by doubling $S_0$ in the studied vessel and decreasing resistance $R$ by the factor of 5. The comparison of calculated (virtual) and measured FFR values is shown in Table 2. All values of the virtual FFR were obtained for stroke volume 65 ml which corresponds to quiet (normal) conditions. One can observe acceptable errors in all cases.

The impact of the heart stroke volume was studied in the second part of the computational experiments. Different heart stroke volumes were applied as boundary condition near the heart: 65 ml, 97.5 ml, and 135 ml. Such increase may be associated with intensive physical activity, hypertension or mental stress. Time profile $Q_H(t)$ (see Fig. 1) was scaled appropriately under the assumption of constant heart rate (1 Hz). Dependence between FFR and cardiac output is presented in Fig. 5.

In Fig. 5 we observe substantial decrease of FFR with increase of the stroke volume. It means that FFR for the patient in quiet conditions with normal heart rate and normal systolic blood flow may be overestimated. Such conditions are likely to be realized outside the hospital and hardly appear during the FFR diagnostics procedure. Long continuous increase in stroke volume may result in heart failure. Thus this factor should be considered by clinicians making decision on invasive or noninvasive stenosis treatment.

Both clinical cases demonstrate that vascular occlusion factor is not the sufficient basis for hemodynamic significance of stenosis. The VOF factors of arteries LCA-1, LAD-1, RCA-2 are between 50–55%. Thus they should

be considered as hemodynamically insignificant cases. Nevertheless, both virtual FFR assessment (0.58) and endovascular measurement (0.51) for LAD-1 (see Table 2) indicate the subcritical values.

Summarizing the results of this and previous research [15] we conclude that variable stroke volume at constant heart rate as well as variable heart rate at constant stroke volume impact the result of the FFR assessment: increase of both factors results in decreased FFR. These physiological conditions are typical for intensive physical activity, psychological stress and some cardiovascular diseases which occur outside the hospital and can not be accounted by traditional diagnostics. The proposed approach is capable to extend this limit and partly assess possible long term stenosis significance.

In addition, the FFR decrease rate (Fig. 5) has no direct correlation with VOF in the case of multiple stenosis. Indeed, we observe similar relative FFR decrease for LCX-1 (VOF = 80%) and LAD-1 (VOF = 50%) as well as for RCA-2 (VOF = 55%) and LAD-2 (VOF = 80%) while almost no changes in LCA-1 (VOF = 55%). This again confirms that VOF value can not be used as a criterion for surgical intervention.

# 3 Discussion

The corner stone of our approach is the usage of limited patient-specific data which are available in every clinic specializing in surgical treatment of coronary vessels. Only angiography and CT data of coronary vessels are needed as personalized input data for our model. Other coefficients correspond to average of physiological ranges rather than patient-specific values. The method can be applied to multiple stenosis cases, in normal and increased stroke volume conditions.

The numerical technique for the virtual FFR assessment in patient-specific coronary network can be used for noninvasive prediction of FFR with acceptable accuracy. However, in some cases only qualitative agreement (error of order 10%) was achieved. This is not sufficient for effective clinical applications.

Several issues affect the accuracy assessment for our approach. First, direct FFR measurements are expensive and still rarely used in clinics and a limited number of cases with required patient-specific data set are available for analysis and validation. Second, measurement errors in clinic may be substantial and may strongly depend on surgeon's qualification. Third, MRI or CT data quality may give rise to substantial segmentation errors and losses in the final vascular 1D structure. In particular, moving coronary vessels feature blurred MRI or CT images. Fourth, mathematical model incompleteness may be essential source of errors. In particular, hydraulic resistance coefficients $R_k$ (1.5) introduced in our model can not be measured directly. In some 1D hemodynamic formulations $R_k$ are not used since Bernoulli integral conservation or pressure continuity in the vessels junctions are imposed instead of (1.5). However, hydraulic resistance coefficients help to account for the impact of the cardiac muscle which performs complex contraction/relaxation and spiral movements. The coefficients $R_k$ are identified by fitting linear velocity in coronary network with well-known physiological values. Such fitting can not produce good accuracy for the patient-specific blood flow using available patient-specific data sets. In defense of our approach we emphasize our interest in the prediction of FFR, the *relative* blood flow characteristic which can be adequately assessed without detailed flow description. In future research we shall study the above issues and provide a rigorous method for the virtual noninvasive FFR assessment.

**Acknowledgment:** The authors acknowledge the staff of I. M. Sechenov First Moscow State Medical University and especially N. Gagarina, E. Fominykh, A. Dzyundzya for the patient-specific data.

**Funding:** The research was supported by the Russian Science Foundation (RSF) grant 14-31-00024.

# References


[1] Y. Adiputra and Sh.-L. Chen, Clinical relevance of coronary fractional flow reserve: art-of-state, *Chinese Med. J.* **128** (2015), No. 10, 1399–1406.

[2] J. Aguado-Sierra, K. H. Parker, J. E. Davies, D. Francis, A. D. Hughes, and J. Mayet, Arterial pulse wave velocity in coronary arteries. In: *Proc. of the 28th IEEE EMBS Annual International Conference*, 2006, pp. 867–870.

[3] E. S. Bernad, S. I. Bernad, and M. L. Craina, Hemodynamic parameters measurements to assess the severity of serial lesions in patient specific right coronary artery. *Bio-Med. Materials Engrg.* **24** (2014), No. 1, 323-334.

[4] E. Boileau and P. Nithiarasu, One-dimensional modelling of the coronary circulation. Application to noninvasive quantification of fractional flow reserve (FFR). *Comp. Exper. Biomed. Sci. Meth. Appl.* **21** (2015), 137–155.

[5] A. Frangi, W. Niessen, K. Vincken, and M. Viergever, Multiscale vessel enhancement filtering. *Medical Image Computing and Computer-Assisted Interventation – MICCAI'98*, *Lecture Notes in Computer Science* **1496** (1998), 130–137.

[6] T. Gamilov, Yu. Ivanov, P. Kopylov, S. Simakov S, and Yu. Vassilevski, Patient specific hemodynamic modelling after occlusion treatment in leg. *Math. Modelling Natur. Pheom.* **9** (2014), No. 6, 85–97.

[7] W. F. Ganong, *Review of Medical Physiology*. Stamford, CT, Appleton and Lange, 1999.

[8] P. D. Morris, D. Ryan, A. C. Morton, et.al., Virtual fractional flow reserve from coronary angiography: modelling the significance of coronary lesions. *JACC: Cardiovascular Interventions* **6** (2013), No. 2, 149–157.

[9] L. Page, B. Riegel, S. B. K. Kern III, et. al., ACC/AHA/SCAI 2005 Guideline update for percutaneous coronary intervention: A report of the American college of cardiology/American heart association task force on practice guidelines. *J. Amer. College Cardiol.* **47** (2006), No. 1, 1–121.

[10] R. Rajani, Y. Wang, A. Uss, et. al., Virtual fractional flow reserve by coronary computed tomography – hope or hype? *EuroIntervention* **9** (2013), No. 2, 277–284.

[11] R. F. Schmidt and G. Thews, *Human Physiology*. Volume 2, 2nd edition, Springer-Verlag, Berlin–Heidelberg, 1989.

[12] S. S. Simakov, T. M. Gamilov, and Y. N. Soe, Computational study of blood flow in lower extremities under intense physical load. *Russ. J. Numer. Anal. Math. Modelling* **28** (2013), No. 5, 485–504.

[13] S. S. Simakov ans A. S. Kholodov, Computational study of oxygen concentration in human blood under low frequency disturbances. *Math. Models Comp. Simul.* **1** (2009), No. 2, 283–295.

[14] C. A. Taylor, T. A. Fonte, and J. K. Min, Computational fluid dynamics applied to cardiac computed tomography for noninvasive quantification of fractional flow reserve. *J. Amer. College Cardiol.* **61** (2013), No. 22, 2233–2241.

[15] Yu. V. Vassilevski, A. A. Danilov, T. M. Gamilov, Yu. A. Ivanov, R. A. Pryamonosov, and S. S. Simakov, Patient-specific anatomical models in human physiology. *Russ. J. Numer. Anal. Math. Modelling* **30** (2015), No. 3, 185–201.

[16] Yu. V. Vassilevski, S. S. Simakov S, V. Yu. Salamatova, Yu. A. Ivanov, and T. D. Dobroserdova, Numerical issues of modelling blood flow in networks of vessels with pathologies. *Russ. J. Numer. Anal. Math. Modelling* **26** (2012), No. 6, 605–622.

[17] M. A. Vis, P. H. Bovendeerd, P. Sipkema, and N. Westerhof, Effect of ventricular contraction, pressure, and wall stretch on vessels at different locations in the wall. *Amer. J. Physiol. Heart Circ. Physiol.* **272** (1997), H2963–H2975.

[18] G. Yang, P. Kitslaar, M. Frenay, J. Dijkstra, et.al., Automatic centerline extraction of coronary arteries in coronary computed tomographic angiography. *Int. J. Cardiovasc. Imaging* **28** (2012), No. 4, 921–933.

[19] Y. E. Yoon and B. K. Koo, Non-invasive functional assessment using computed tomography: when will they be ready for clinical use? *Cardiovasc. Diagnosis Therapy* **2** (2012), No. 2, 106–112.

[20] C. K. Zarins, C. A. Taylor, and J. K. Min, Computed fractional flow Reserve (FFTCT) derived from coronary CT angiography *J. Cardiovasc. Transl. Research* **6** (2013), No. 5, 708–714.

[21] J.-M. Zhang, T. Luo, S.Y. Tan, et.al. Hemodynamic analysis of patient-specific coronary artery tree, *Int. J. Numerical Meth. Biomed. Engrg.* (2015), DOI: 10.1002/cnm.2708.